

available at www.sciencedirect.comwww.elsevier.com/locate/brainres
**BRAIN
RESEARCH**

Research Report

Effects of systemic PSI administration on catecholaminergic cells in the brain, adrenal medulla and carotid body in Wistar rats

Alexander Hawlitschka^a, Stefan J.P. Haas^a, Oliver Schmitt^{a,*},
Dieter G. Weiss^b, Andreas Wree^a

^aInstitute of Anatomy, Faculty of Medicine, University of Rostock, POB 100888, 18055 Rostock, Germany

^bInstitute of Biological Sciences, Cell Biology and Biosystems Technology, University of Rostock, D-18051 Rostock, Germany

ARTICLE INFO

Article history:

Accepted 31 July 2007

Available online 14 August 2007

Keywords:

Parkinson's disease
Neurodegeneration
Substantia nigra
Olfactory bulb
Blood brain barrier

ABSTRACT

Traditional Parkinson's disease models in rats have several disadvantages. A promising alternative in terms of a more physiological model was proposed by McNaught et al. [McNaught, K.S., Perl, D.P., Brownell, A.L., Olanow, C.W., 2004. Systemic exposure to proteasome inhibitors causes a progressive model of Parkinson's disease. *Ann. Neurol.* 56, 149–162.] inhibiting the proteasomal protein degradation in vivo where they observed in Sprague–Dawley rats distinct symptoms of Parkinson's disease, a typical slow progredient loss of dopaminergic neurons in the substantia nigra and a lack of dopaminergic afferences in the striatum. We administered to Wistar rats a synthetic proteasome inhibitor (PSI) analogous to the published method. Locomotor changes were analysed by a footprint test. Brain slices containing the substantia nigra and the striatum were stained immunohistochemically against tyrosine hydroxylase, neuronal nuclei antigen, glial fibrillary acidic protein, α -synuclein and microglia. Standard histological stainings (haematoxylin eosin or Nissl) were also performed. The proteasome inhibitor effect on the glomerular layer of the olfactory bulb, the adrenal medulla and the carotid body was examined. We observed no PSI-induced motor deficits and loss of tyrosine hydroxylase immunoreactivity in the substantia nigra or the striatum. However, we detected a distinct increase of tyrosine hydroxylase immunoreactivity in the glomerular layer of the olfactory bulb and in the adrenal medulla. Our results fall in line with reports of other research groups which failed to reproduce the original report, but here for the first time McNaughts model could not be reproduced in Wistar rats. The observed effects on the olfactory bulb and peripheral catecholaminergic organs speak for an impermeability of the blood brain barrier for PSI.

© 2007 Elsevier B.V. All rights reserved.

* Corresponding author. Fax: +49 381 4948402.

E-mail address: schmitt@med.uni-rostock.de (O. Schmitt).

Abbreviations: 6-OHDA, 6-hydroxydopamine; BW, body weight; CPu, caudate-putamen; DAB, 3,3'-diaminobenzidine hydrochloride; ETOH, ethanol; GFAP, glial fibrillary acidic protein; HE, haematoxylin eosin; ir, immunoreactivity; NeuN, neuron-specific nuclear protein; OD, optical density; PD, Parkinson's disease; PSI, synthetic proteasome inhibitor (Z-lle-Glu(OtBu)-Ala-Leu-al N-benzyloxycarbonyl-L-isoleucyl-gamma-t-butyl-L-glutamyl-L-alanyl-L-leucinal); SEM, standard error of mean; SN, substantia nigra; SNC, pars compacta of the substantia nigra; TH, tyrosine hydroxylase

1. Introduction

Parkinson's disease (PD) is the second most abundant neurodegenerative disorder with a rising clinical and social relevance due to demographic aging. A progressive ongoing loss of dopaminergic neurons in the pars compacta of the substantia nigra (SNc) leads to the clinical features of rigor, tremor and akinesia. This neuronal loss is accompanied by a strong reduction of neurons in the locus coeruleus, dorsal motor nucleus of the vagus, and the nucleus basalis of Meynert (Braak et al., 2003, 2004; Wolters and Braak, 2006; Zarow et al., 2003).

The traditional neurotoxic animal models of PD have a number of shortcomings, like unphysiological progress and a lack of specificity of neurotoxicity (Schober, 2004). A positive aspect of 6-hydroxydopamine (6-OHDA) neurotoxicity is its reliable applicability also with regard to other neurotoxic Parkinsonian animal models. However, its rapid and unphysiological effect of neuronal death has raised criticism (Gerlach et al., 2007; Tolwani et al., 1999; Melrose et al., 2006). With regard to stereotactic cell transplantation experiments, the 6-OHDA model may affect other central metabolic, neuronal and/or glial systems which may influence the graft in an unknown way. The MPTP model also shows acute and non-progressive dopaminergic cell death. Furthermore, this model works well only in the C57BL/6 mice strain and is less effective in other mice strains and rats (Gerlach and Riederer, 1996). Moreover, inclusion bodies could rarely be found. It is also possible to induce dopaminergic neuronal cell death by application of rotenone, but the specificity of this model is discussed still controversial. The successful application of rotenone is technically challenging because of the need of continuous injection in the jugular vein by osmotic mini pumps (Betarbet et al., 2000). Moreover, it is supposed that there is an intra-strain variability in susceptibility to rotenone and MPTP (Melrose et al., 2006; Gerlach and Riederer, 1996). The administration of the herbicide paraquat and the combined adminis-

tration of paraquat and the fungicide maneb to mice leads to a loss of dopaminergic neurons in the SN, but paraquat does not cross the blood brain barrier offhandedly (Gerlach and Riederer, 1996). The models of paraquat, paraquat maneb and rotenone lead to a high mortality because a high systemic toxicity (Cicchetti et al., 2005; Melrose et al., 2006) is induced. Then less of 50% of surviving animals treated with rotenone develop consistent lesions (Dawson et al., 2002). Therefore, much effort has been spent to establish a more physiological Parkinsonian animal model with gradually extending neuropathologic signs.

The reports of McNaught et al. (2002a,b, 2004) and other research groups (Schapira et al., 2006; Zeng et al., 2006) have provided evidence that the systemic administration of proteasome inhibitors to rodents and the subsequent disturbance of the ubiquitin-dependent protein degradation could be a revolutionary new model with typical progressive dopaminergic cell loss in the SNc, inclusion bodies and behavioural deficits (Chung et al., 2001; Kikuchi et al., 2003; Mytilineou et al., 2004; Rideout et al., 2005; Sawada et al., 2004). Nevertheless, there are several reports which fail to reproduce this model in Sprague-Dawley rats and mice (Bové et al., 2006; Kordower et al., 2006; Manning-Bog et al., 2006). This gave rise to a substantial controversial discussion of these different results. The objective of this contribution was to establish this new model in Wistar rats and to investigate the effect of a proteasome inhibitor on peripheral catecholaminergic organs.

2. Results

2.1. Bodyweight measurement and assessment for motor dysfunction

Injections of PSI and ETOH were well tolerated by both groups. However, PSI and ETOH rats developed subcutaneous

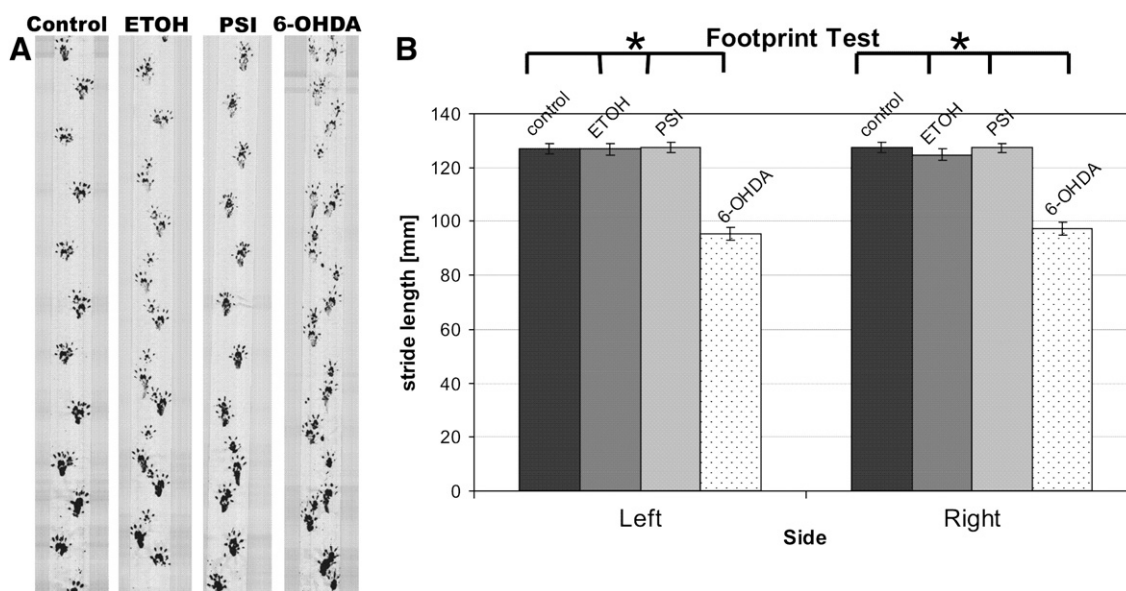


Fig. 1 – Behavioural analysis of motor dysfunctions in PSI-rats. (A) Footprint test 2 months after last PSI administration. Examples for traces left by ink dyed paws of rats. The reduction of the stride length of 6-OHDA-hemilesioned rats is clearly visible. (B) Values shown are means ($n=8$ or 9 per group) \pm standard error of mean (SEM). * $P<0.05$.

hardening on injection sites. During the experiment, rats exhibited no significant differences in bodyweight compared to control rats.

According to footprint analysis, PSI rats showed no motor deficits compared to ETOH rats or control rats, even 2 months after the last injections. There were no significant differences in the stride length between PSI rats ($127 \text{ mm} \pm 1.68 \text{ mm}$), ETOH rats ($125 \text{ mm} \pm 2.17 \text{ mm}$) and totally untreated control rats ($127 \text{ mm} \pm 1.98 \text{ mm}$). However, a significant shortening of about 30% in stride length in 6-OHDA rats ($96.3 \text{ mm} \pm 2.3 \text{ mm}$) was measured (Figs. 1A, B).

2.2. Histological and stereological assessment of the brain

Examination of Nissl and HE stainings revealed no obvious differences of morphologic structures like cell bodies and nuclei. Loss of cells, gliosis, intracellular changes (cytoplasmic inclusion bodies like Lewy bodies (Ardley et al., 2003))

and fragmented nuclei were not found in any stainings of ETOH and PSI rats. Immunohistochemical staining against α -synuclein revealed no differences between PSI rats and ETOH rats. No inclusion bodies were detected, whereas in control slices of the midbrain of a PD patient α -synuclein-positive inclusion bodies could be found numerously (Figs. 5A, B). Remarkably in dopaminergic structures of the brain like the SN and the glomerular layer of the olfactory bulb in PSI and in ETOH rats the immunoreactivity for α -synuclein was increased (Figs. 5C, D, E, F) and several cell bodies were marked clearly in the ventral tegmental area (not shown) and in the glomerular layer of the olfactory bulb (Figs. 5G, H, I, J).

The densitometric analysis of TH-ir of the CPu and the SN gave no clues of a dopaminergic injury. Neither in the CPu nor in the SN significant differences of TH-ir between ETOH and PSI rats were detectable. The mean ODs of the CPu slices were $14.57\% \pm 1.62\%$ in ETOH rats and $14.08\% \pm 0.816\%$ in PSI rats. The mean ODs of SN slices were $24.42\% \pm 1.27\%$ in ETOH rats

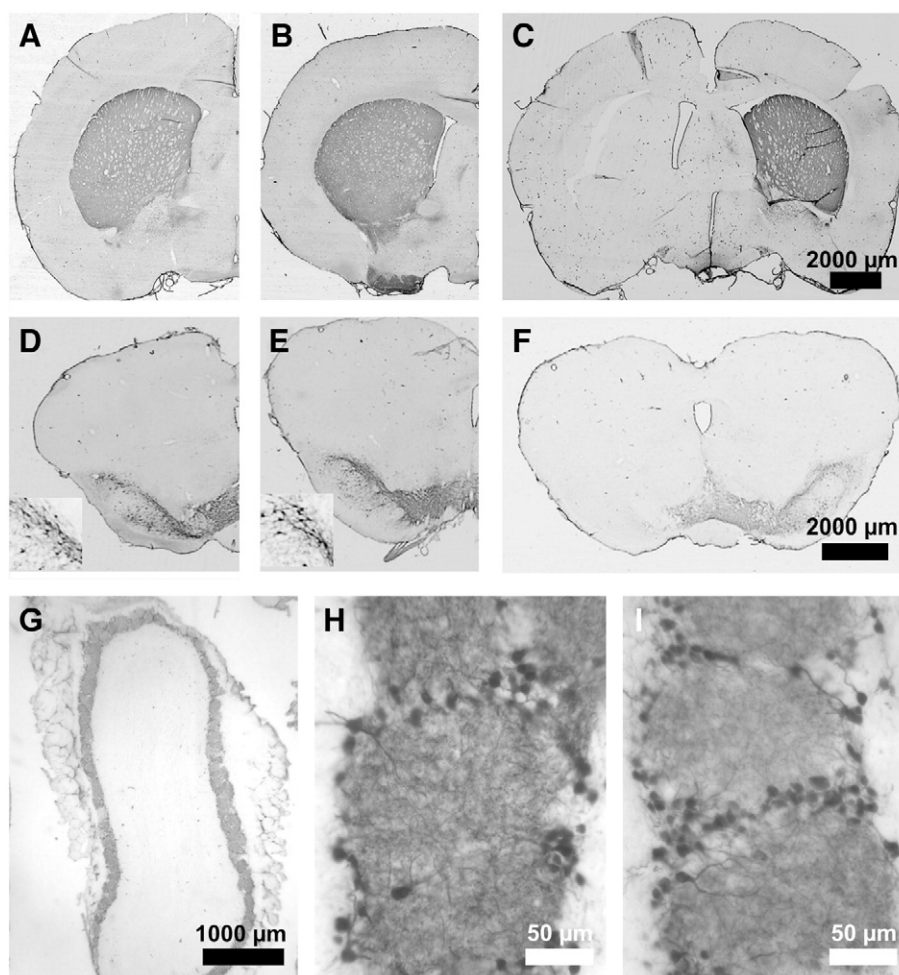


Fig. 2 – Analysis of TH content in the CPu, the SN and the olfactory bulb. (A, B, C) No differences in the content of TH-positive fibres in the CPu between PSI rats (A) and ETOH rats (B) are detectable but in hemilesioned 6-OHDA rats (C) there is a distinct loss of TH immunoreactivity visible at the lesioned side (left hemisphere). (D, E, F) In the SN, no differences in the content of TH in PSI rats (D) and ETOH rats (E) are visible, but at the lesioned side of hemilesioned rats TH-positive neurons vanished (insets in D and E: higher power images of the pars compacta of the SN). (G, H, I) Measurement of OD in the glomerular layer of olfactory bulb (G overview of an anti-TH-stained frontal section of the olfactory bulb) of PSI rats (H) revealed a higher content of TH than in ETOH rats (I).

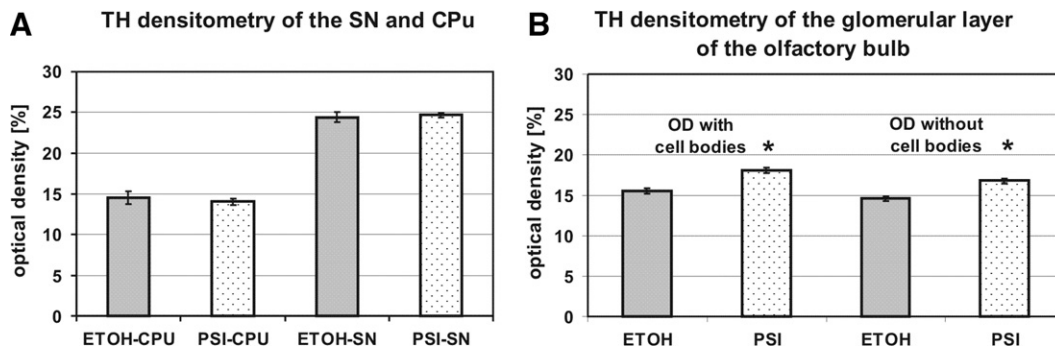


Fig. 3 – Measurement of OD in immunostainings against TH. No differences between PSI and ETOH rats in the CPU and the SN in TH content were found (A) but significant enhancement of TH content in the glomerular region of PSI rats was measured (B). Values shown are means ($n=6$) \pm standard error of mean (SEM). * $P<0.05$.

and $24.68\% \pm 0.58\%$ in PSI rats (Figs. 2A, B, D, E; Fig. 3A). In contrast, a unilateral 6-OHDA lesion led to a massive loss of TH-ir in the ipsilateral SN and CPU (Figs. 2C, F).

Interestingly, in the glomerular layer of the olfactory bulb significant differences in the TH content were found between PSI and ETOH rats (Figs. 2G, H, I). PSI rats exhibited higher levels of TH-ir. Including somata in the analysis, the OD in the glomerular layer of PSI rats averaged $18.03\% \pm 0.33\%$ and $15.56\% \pm 0.35\%$ in ETOH rats. Excluding cell bodies in the measurement, the OD averaged $16.76\% \pm 0.27\%$ in PSI rats and $14.64\% \pm 0.29\%$ in ETOH rats (Figs. 2H, I; Fig. 3B).

2.3. Histological and stereological assessment of peripheral catecholaminergic organs

In the adrenal medulla of PSI rats (Figs. 5K, L), the OD measurement of sections stained against TH revealed a significant increase of TH (Figs. 4A–D). The mean OD of adrenal medulla was $4.59\% \pm 0.13\%$ for ETOH rats and $5.19\% \pm 0.14\%$ for PSI rats (Fig. 4J). Nevertheless, the stereologic estimates of the volumes provided no evidence for alterations of the adrenal medulla or the adrenal cortex following PSI injection (Fig. 4I).

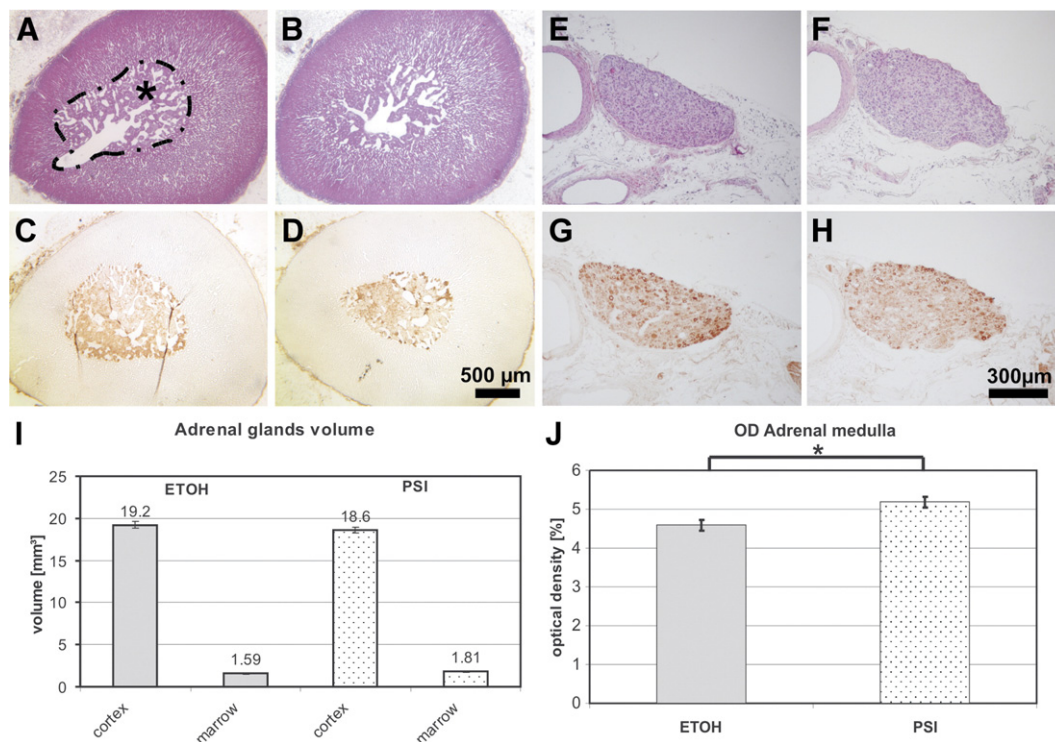


Fig. 4 – Analysis of peripheral catecholaminergic organs. (A, B, C, D) Adrenal gland, (A) HE staining of a PSI rat (*: adrenal medulla), (B) of an ETOH rat, (C) anti-TH staining of a PSI rat and (D) of an ETOH rat. (E, F, G, H) Carotid bodies, (E) HE staining of a PSI rat, (F) of an ETOH rat, (G) anti-TH staining of a PSI rat and (H) of an ETOH rat. (I) Values shown are means of volume of cortex and medulla of the adrenal glands ($n=6$ per group) \pm SEM. (J) Means of the optical density (OD) of anti-TH stained slices of the adrenal medulla ($n=6$ per group) \pm SEM. * $P<0.05$.

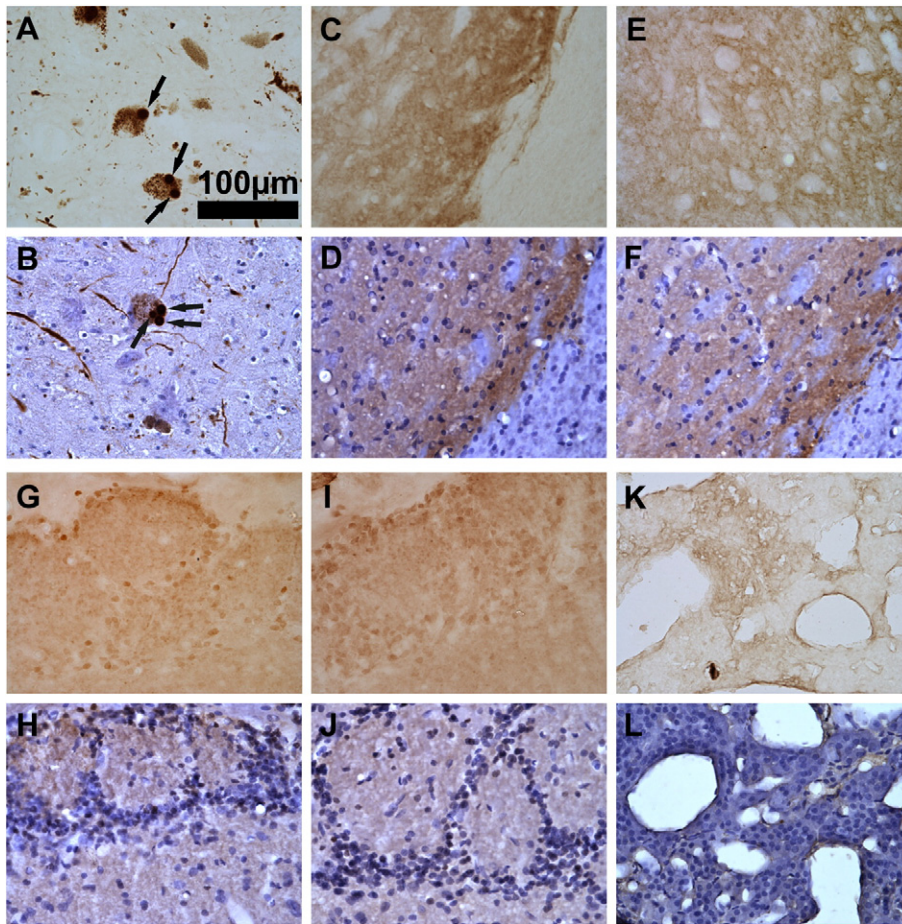


Fig. 5 – Immunohistochemically stained sections of brain and adrenal medulla against α -synuclein. (A, B) SN of a deceased PD patient with clearly recognizable intracellular inclusion bodies (arrows), (C, D) SN of a PSI rat, (E, F) SN of an ETOH rat, (G, H) glomerular layer of a PSI rat and (I, J) an ETOH rat and (K, L) the adrenal medulla of a PSI rat. Each second slice stained against α -synuclein was counterstained with haematoxylin (B, D, F, H, J, L). In contrast to the Parkinsonian SN no inclusion bodies were detectable in the rat tissues.

Inspecting the carotid bodies, no obvious differences between the ETOH and PSI rats were observed (Figs. 4E–H).

3. Discussion

With regard to behavioural assessment, histological, immunohistochemical stainings and quantitative analysis the findings of McNaught et al. (2004) could not be reproduced. Neither a reduced TH-ir in the CPu or in the SN nor behavioural deficits were found in PSI rats. Eosinophilic or α -synuclein-ir inclusion bodies were not detected in catecholaminergic cells of all examined brain structures and organs. Similar problems in reproducing the results of McNaught et al. (2004) were reported by independent research groups (Bové et al., 2006; Kordower et al., 2006; Manning-Bog et al., 2006).

Dissolution and application of PSI were carried out strictly to Dr. McNaughts recommendations. Here, we cannot exclude that the differences of our results and those of McNaught et al. (2004) may be due to differences in rat strains since we performed experiments with the Wistar strain, and not with Sprague–Dawley rats. However, others reported successful induction of

neuronal cell loss in the SN and behavioural deficits in Wistar rats after applying proteasome inhibitors (Zeng et al., 2006).

These contradicting observations demand further discussion. It is possible that the lots of PSI vary with regard to purity and quality. Here, we used PSI from Bachem (Weil am Rhein, Germany) whereby Dr. McNaughts group obtained PSI from Sigma-Aldrich Corp (St. Louis, MO). Also the solvents and the vehicles could have influenced successful induction of PD-like symptoms in rats via PSI application (McNaught et al., 2004; Schapira et al., 2006; Zeng et al., 2006) unfortunately the composition and purity level of their solvent ethanol were not specified.

It is possible that PSI could not pass the blood brain barrier of Wistar rats, since we were able to detect changes only in catecholaminergic structures of PSI rats which were not or insufficiently protected by a blood organ barrier. To be specific, an increase of TH content was found in the adrenal medulla and the glomerular layer of the olfactory bulb by measuring the OD. The latter is in agreement with the increase of dopaminergic cell numbers in the olfactory bulb of patients having symptoms of PD or in 6-OHDA lesion models (Huisman et al., 2004; Winner et al., 2006). Braak et al. (2003, 2004, 2006)

characterised a sixfold staging of PD. In presymptomatic stages one and two the first conspicuous morphologic features are detectable among others in the olfactory bulb. So it could not be excluded that our PSI rats reached a stage analogue to a presymptomatic stage one or two of human PD. Moreover, in the primate MPTP model, dopamine and noradrenaline were substantially elevated in the adrenal medulla (Fine et al., 1985). Interestingly, both structures are not (adrenal medulla) or insufficiently (olfactory bulb) protected by a blood organ barrier. Likewise, due to this morphologic difference, the uptake of MPTP in the brain through the olfactory bulb by nasal application (Pearce et al., 1995) was explained. Surprisingly, the effects observed here in the olfactory bulb and in the adrenal medulla after systemic administration of PSI induced the preclinical feature of an elevated TH-ir but lacking the effects reported for the SN, locus coeruleus and nucleus basalis of Meynert by McNaught et al. (2004). For these structures massive neuronal cell degeneration was observed. If the solvents were impure (the ethanol could be denatured by additives), the mixture may have influenced the blood brain barrier and facilitated PSI to pass. Perhaps impure solvents instead of PSI are responsible for the described effects to neurons. Landau et al. (2007) provide an indication for this hypothesis. They reported a loss of dopamine- and TH-positive cells in the SN of C57BL/6 mice which were treated with PSI but also in mice which were injected with solvents (70% ETOH) only. However, totally untreated mice did not develop such a dopaminergic cell loss.

So far, in the light of controversial studies and the results observed in our laboratory, the PSI application that was expected to model a progressive Parkinsonian syndrome with distinct neuropathological signs is not reproducible. More efforts need to be spent on understanding transport and metabolic effects on a completely defined PSI solution from the subcutaneous site, over the blood brain barrier and to its targets: the dopaminergic cell population.

4. Experimental procedure

4.1. Rats and treatments

25 Male Wistar rats (~200 g) were obtained from Charles River (Sulzfeld, Germany). Animals were kept at 22 °C at 12-h light-dark cycle with free access to food and water. Experiments were performed according to standard legal guidelines and were approved by the local government authorities.

The proteasome inhibitor PSI (Bachem, Weil am Rhein, Germany) was dissolved and handled exactly in the same way as recommended by Dr. K. McNaught (personal communication). The solution of PSI was prepared freshly prior to injection. Firstly, 5 mg PSI was dissolved in 875 µl absolute ethanol (ETOH) and then filled up with 375 µl H₂O, to obtain a solution of 4 µg PSI/µl 70% ethanol. We draw attention, that the ethanol used was pure and not denatured.

Eight rats were injected with 3.0 mg/kg PSI (0.75 µl/g body-weight, s.c.; PSI rats), and as sham controls, eight animals were injected with vehicle only (70% ethanol, s.c.; ETOH rats). The injections were made six times over a period of 2 weeks (Mon, Wed, Fri, Mon, Wed, Fri). Additionally, for the footprint test, nine totally untreated age-matched control rats (control

rats) and nine 6-OHDA-hemilesioned rats (6-OHDA rats) were tested. 6-OHDA rats were generated by lesion of the right substantia nigra (SN) via stereotaxic injection of 26 µg 6-OHDA (Sigma) in 4 µl of a solution of 0.9% NaCl, 0.8 µg/µl Ascorbic acid (Merck) over 4 min into the right medial forebrain bundle (coordinates according to bregma: AP -2.3; L -1.5; V -8.5) (Paxinos, 1998). Prior lesion, rats were narcotised with pentobarbital (4.5 mg/100 g BW in 0.9% NaCl). Successfully lesioned rats exhibited more than 4 contralateral rotations/min over 40 min after apomorphine injection (0.25 mg/kg BW; s.c.).

Two months after the last PSI injections or at corresponding time points for control rats, animals were killed by pentobarbital (5 mg/100 g in 0.9% NaCl) and perfused transcardially with 50 ml 0.9% NaCl solution followed by 400 ml 4% paraformaldehyde (in phosphate-buffered saline, 0.1 M, pH 7.4).

4.2. Bodyweight measurement and assessment of motor dysfunction

Rats, including control rats, were weighted daily after application of PSI or 70% ethanol as well as 1 month after the last injection and at the day of perfusion, 2 months after the last injections of PSI or vehicle.

Two weeks prior, during and following the injections of PSI and ETOH all rats were trained to run through an acrylic glass channel carpeted with a bar of paper (length: 96 cm, wide: 5.7 cm). Also control rats and 6-OHDA rats underwent this training. One day before the perfusion animals paws were dyed with ink. Each animal was allowed to run across a bar of paper through the acrylic glass channel to document the footstep patterns (Metz et al., 2005).

4.3. Examined brain regions, peripheral organs and immunostaining

Brains were postfixed for 4 hrs, cryoprotected overnight in 20% sucrose, frozen in isopentane (-50 °C) and stored at -80 °C. Serial cryostat sections (30 µm) were made. Regions containing the substantia nigra (SN), the caudate-putamen (CPu) and the olfactory bulbs were stained.

Brain sections were processed immunohistochemically against TH (1:1000, Sigma-Aldrich), activated microglia (Ox42, 1:800, Chemicon), NeuN (1:500, Chemicon), α -synuclein (1:2000, BD Biosciences) or glial fibrillary acidic protein (GFAP, 1:400, Sigma-Aldrich). The reaction was visualised with a standardised 3,3'-diaminobenzidine hydrochloride (10 mg/100 ml phosphate-buffered saline, DAB, Sigma-Aldrich) procedure using the avidin biotin complex (ABC) immunostaining kit (Vector). Furthermore, parallel brain sections were stained with haematoxylin eosin (HE) or with cresyl violet acetate 0.1% (Nissl). As positive control for the α -synuclein stainings, 7-µm-thick paraffin midbrain slices of a deceased PD patient, which were provided by courtesy of Prof. Braak (Institute of Anatomy, Johann Wolfgang Goethe University of Frankfurt am Main), were stained immunohistochemically against α -synuclein and counterstained with haematoxylin (Fig. 5).

The adrenal glands and the carotid bodies were embedded in paraffin and cut into 7-µm-thick sections to examine the histology of the organs and the catecholaminergic chromaffine cells by TH immunohistochemistry. Additional slices of adrenal

medulla also underwent an immunohistochemical procedure against α -synuclein.

4.4. Quantitative and histological analysis

The immunoreactivity can be quantified by calculating the optical density (OD) (Schmitt et al., 2004). The OD is calculated by correcting the unspecific background to allow comparisons and determining the mean ODs of different sections of the same animal.

To measure the OD of TH-ir in SNC and CPU, the DAB visualised sections were digitised by scanning in transmission mode using a high performance scanner (Nexscan F4100, Heidelberg). Measurement of the OD in the digital images was realised with Matlab 6.0® (MathWorks) in interactively defined regions of interest. The measurement of the OD in anti-TH DAB stainings of the glomerular layer of the olfactory bulb and the adrenal medulla were similar but digital images for densitometric analysis were obtained by light microscopy (Leitz Aristoplan, Ernst Leitz, Wetzlar GmbH) with a digital camera (SPOT 7.3. Three Shot Color, Diagnostic Instruments Inc.). The calculation of OD in the glomerular layer was performed in two ways: (a) with and (b) without cell bodies to detect compartmental dependent differences of cell bodies or nerve fibres with the same method. In the latter case only TH-ir nerve fibres were considered.

The total volume of adrenal glands and of adrenal medulla was determined by the method of Cavalieri (Gundersen et al., 1988). For this, a microscopic picture of every eleventh slice of the HE-stained structure was projected on a special grid of points, and the points which overlapped with the projection of the structure were counted.

4.5. Statistics

All values are stated as mean \pm SEM (standard error of mean) in tables and diagrams. The statistical analysis was carried out by Mann and Whitney *U*-test, and Wilcoxon test with SPSS® 11.0 (level of significance of $p \leq 0.05$).

Acknowledgments

We thank F. Winzer and A. Schümann of the Institute of Anatomy (University of Rostock) for their excellent histologic preparations and Mr. U. Haase who constructed the channel for stride length analysis, as well as Prof. R. Köhling (Institute of Physiology, University of Rostock) for his critical discussion. Especially we thank Prof. H. Braak (Institute of Anatomy, Johann Wolfgang Goethe University of Frankfurt am Main) for supporting us with brain tissue from a Parkinson patient and for his important advices.

REFERENCES

- Ardley, H.C., Scott, G.B., Rose, S.A., Tan, N.G.S., Markham, A.F., Robinson, P.A., 2003. Inhibition of proteasomal activity causes inclusion formation in neuronal and non-neuronal cells overexpressing parkin. *Mol. Biol. Cell* 14, 4541–4556.
- Betarbet, R., Sherer, T.B., MacKenzie, G., Garcia-Osuna, M., Panov, A.V., Greenamyre, J.T., 2000. Chronic systemic pesticide exposure reproduces features of Parkinson's disease. *Nat. Neurosci.* 3, 1301–1306.
- Bové, J., Zhou, C., Jackson-Lewis, V., Taylor, J., Chu, Y., Rideout, H.J., Wu, D.C., Kordower, J.H., Petrucelli, L., Przedborski, S., 2006. Proteasome inhibition and Parkinson's disease modeling. *Ann. Neurol.* 60, 260–264.
- Braak, H., Tredici, K.D., Rüb, U., de Vos, R.A., Jansen Steur, E.N., Braak, E., 2003. Staging of brain pathology related to sporadic Parkinson's disease. *Neurobiol. Aging* 24, 197–211.
- Braak, H., Ghebremedhin, E., Rüb, U., Bratzke, H., Tredici, K.D., 2004. Stages in the development of Parkinson's disease-related pathology. *Cell Tissue Res.* 318, 121–134.
- Braak, H., Bohl, J.R., Müller, C.M., Rüb, U., de Vos, R.A.I., Tredici, K.D., 2006. Stanley Fahn Lecture 2005: the staging procedure for the inclusion body pathology associated with sporadic Parkinson's disease reconsidered. *Mov. Disord.* 21, 2042–2051.
- Chung, K.K., Dawson, V.L., Dawson, T.M., 2001. The role of the ubiquitin-proteasomal pathway in Parkinson's disease and other neurodegenerative disorders. *Trends Neurosci.* 24, 7–14.
- Cicchetti, F., Lapointe, N., Roberge-Tremblay, A., Saint-Pierre, M., Jimenez, L., Ficke, B.W., Gross, R.E., 2005. Systemic exposure to paraquat and maneb models early Parkinson's disease in young adult rats. *Neurobiol. Dis.* 20, 360–371.
- Dawson, T.M., Mandir, A.S., Lee, M.K., 2002. Animal models of PD: pieces of the same puzzle? *Neuron* 35, 219–222.
- Fine, A., Reynolds, G.P., Nakajima, N., Jenner, P., Marsden, C.D., 1985. Acute administration of 1-methyl-4-phenyl-1,2,3,6-tetrahydropyridine affects the adrenal glands as well as the brain in the marmoset. *Neurosci. Lett.* 58, 123–126.
- Gerlach, M., Riederer, P., 1996. Animal models of Parkinson's disease: an empirical comparison with the phenomenology of the disease in man. *J. Neural Transm.* 103, 987–1041.
- Gerlach, M., Reichmann, H., Riederer, P., Dietmaier, O., Götz, W., Laux, G., Storch, A., 2007. Die Parkinson-Krankheit: Grundlagen, Klinik, Therapie, 4th Ed. Springer, Wien, pp. 105–136.
- Gundersen, H.J., Bendtsen, T.F., Korbo, L., Marcussen, N., Moller, A., Nielsen, K., Nyengaard, J.R., Pakkenberg, B., Sorensen, F.B., Vesterby, A., West, M.J., 1988. Some new, simple and efficient stereological methods and their use in pathological research and diagnosis. *A.P.M.I.S.* 96, 379–394.
- Huisman, E., Uylings, H.B., Hoogland, P.V., 2004. A 100% Increase of dopaminergic cells in the olfactory bulb may explain hyposmia in Parkinson's disease. *Mov. Disord.* 19, 687–692.
- Kikuchi, S., Shinpo, K., Tsuji, S., Takeuchi, M., Yamagishi, S., Makita, Z., Niino, M., Yabe, I., Tashiro, K., 2003. Effect of proteasome inhibitor on cultured mesencephalic dopaminergic neurons. *Brain Res.* 964, 228–236.
- Kordower, J.H., Kanaan, N.M., Chu, Y., Suresh Babu, R., Stansell III, J., Terpstra, B.T., Sortwell, C.E., Steece-Collier, K., Collier, T.J., 2006. Failure of proteasome inhibitor administration to provide a model of Parkinson's disease in rats and monkeys. *Ann. Neurol.* 60, 264–268.
- Landau, A.M., Kouassi, E., Siegrist-Johnstone, R., Desbarats, J., 2007. Proteasome inhibitor model of Parkinson's disease in mice is confounded by neurotoxicity of the ethanol vehicle. *Mov. Disord.* 22, 403–407.
- Manning-Bog, A.B., Reaney, S.H., Chou, V.P., Johnston, L.C., McCormack, A.L., Johnston, J., Langston, J.W., Di Monte, D.A., 2006. Lack of nigrostriatal pathology in a rat model of proteasome inhibition. *Ann. Neurol.* 60, 256–260.
- McNaught, K.S., Mytilineou, C., JnoBaptiste, R., Yabut, J., Shashidharan, P., Jennert, P., Olanow, C.W., 2002a. Impairment of the ubiquitin-proteasome system causes dopaminergic cell death and inclusion body formation in ventral mesencephalic cultures. *J. Neurochem.* 81, 301–306.
- McNaught, K.S., Björklund, L.M., Belizaire, R., Isacson, O., Jenner, P., Olanow, C.W., 2002b. Proteasome inhibition causes nigral

- degeneration with inclusion bodies in rats. *Neuroreport* 13, 1437–1441.
- McNaught, K.S., Perl, D.P., Brownell, A.L., Olanow, C.W., 2004. Systemic exposure to proteasome inhibitors causes a progressive model of Parkinson's disease. *Ann. Neurol.* 56, 149–162.
- Melrose, H.L., Lincoln, S.J., Tyndall, G.M., Farrer, M.J., 2006. Parkinson's disease: a rethink of rodent models. *Exp. Brain Res.* 173, 196–204.
- Metz, G.A., Tse, A., Ballermann, M., Smith, L.K., Fouad, K., 2005. The unilateral 6-OHDA rat model of Parkinson's disease revisited: an electromyographic and behavioural analysis. *Eur. J. Neurosci.* 22, 735–744.
- Mytilineou, C., McNaught, K.S., Shashidharan, P., Yabut, J., Baptiste, R.J., Parnandi, A., Olanow, C.W., 2004. Inhibition of proteasome activity sensitizes dopamine neurons to protein alterations and oxidative stress. *J. Neural Transm.* 111, 1237–1251.
- Paxinos, G., 1998. *The Rat Brain in Stereotaxic Coordinates*. Academic Press, San Diego.
- Pearce, R.K., Hawkes, C.H., Daniel, S.E., 1995. The anterior olfactory nucleus in Parkinson's disease. *Mov. Disord.* 10, 283–287.
- Rideout, H.J., Lang-Rollin, I.C., Savalle, M., Stefanis, L., 2005. Dopaminergic neurons in rat ventral midbrain cultures undergo selective apoptosis and form inclusions, but do not up-regulate iHSP70, following proteasomal inhibition. *J. Neurochem.* 93, 1304–1313.
- Sawada, H., Kohno, R., Kihara, T., Izumi, Y., Sakka, N., Ibi, M., Nakanishi, M., Nakamizo, T., Yamakawa, K., Shibasaki, H., Yamamoto, N., Akaike, A., Inden, M., Kitamura, Y., Taniguchi, T., Shimohama, S., 2004. Proteasome mediates dopaminergic neuronal degeneration, and its inhibition causes α -synuclein inclusions. *J. Biol. Chem.* 279, 10710–10719.
- Schapira, A.H.V., Cleeter, M.W.J., Muddle, J.R., Workman, J.M., Cooper, J.M., King, R.H.M., 2006. Proteasomal inhibition causes loss of nigral tyrosine hydroxylase neurons. *Ann. Neurol.* 60, 253–254.
- Schmitt, O., Preuß, S., Haas, S.J.P., 2004. Comparison of contrast, sensitivity and efficiency of signal amplified and nonamplified immunohistochemical reactions suitable for videomicroscopy-based quantification and neuroimaging. *Brain Res. Protoc.* 12, 157–171.
- Schober, A., 2004. Classic toxin-induced animal models of Parkinson's disease: 6-OHDA and MPTP. *Cell Tissue Res.* 318, 215–224.
- Tolwani, R.J., Jakowec, M.W., Petzinger, G.M., Green, S., Waggle, K., 1999. Experimental models of Parkinson's disease: insights from many models. *Lab. Anim. Sci.* 49, 363–371.
- Winner, B., Geyer, M., Couillard-Despres, S., Aigner, R., Bogdhan, U., Aigner, L., Kuhn, G., Winkler, J., 2006. Striatal deafferentation increases dopaminergic neurogenesis in the adult olfactory bulb. *Exp. Neurol.* 197, 113–121.
- Wolters, E.C., Braak, H., 2006. Parkinson's disease: premotor clinico-pathological correlations. *J. Neural Transm.* 70, 309–319.
- Zarow, C., Lyness, S.A., Mortimer, J.A., Chui, H.C., 2003. Neuronal loss is greater in the locus coeruleus than nucleus basalis and substantia nigra in Alzheimer and Parkinson's diseases. *Arch. Neurol.* 60, 337–341.
- Zeng, B.Y., Bukhatwa, S., Hikima, A., Rose, S., Jenner, P., 2006. Reproducible nigral cell loss after systemic proteasomal inhibitor administration to rats. *Ann. Neurol.* 60, 248–252.